

Noise Distribution Adaptive Self-Supervised Image Denoising using Tweedie Distribution and Score Matching

Kwanyoung Kim¹ Taesung Kwon¹ Jong Chul Ye^{1,2,3}

¹ Department of Bio and Brain Engineering

² Kim Jaechul Graduate School of AI

³ Department of Mathematical Sciences

Korea Advanced Institute of Science and Technology (KAIST)

{cubeyoung, star.kwon, jong.ye}@kaist.ac.kr

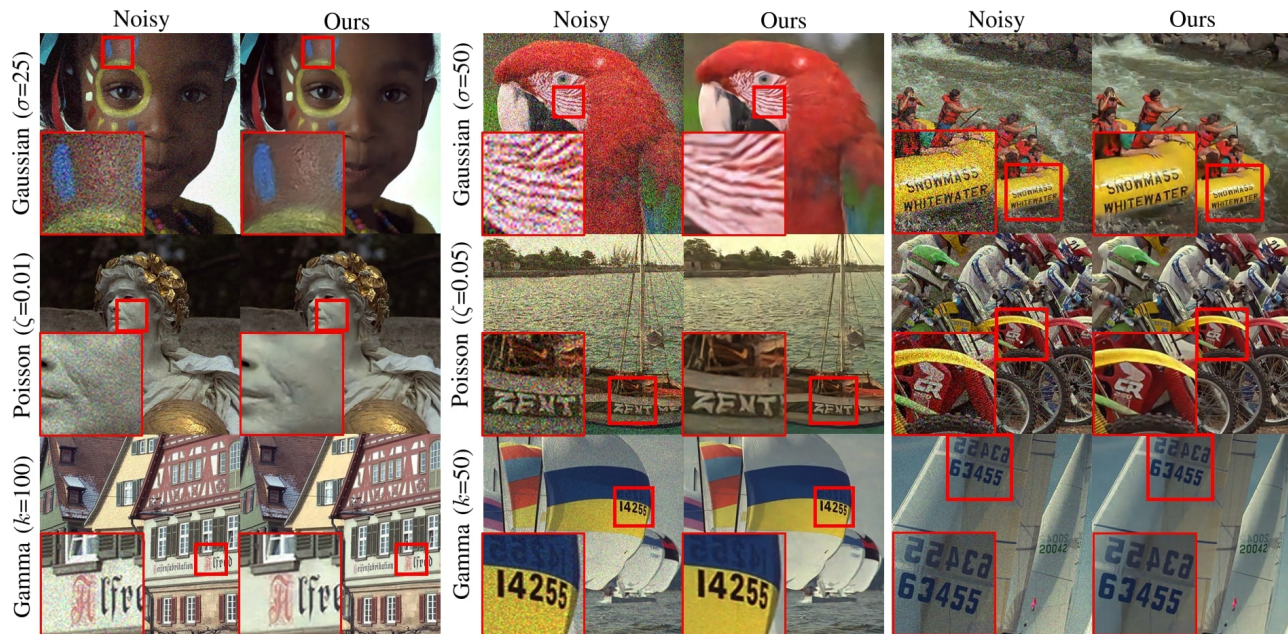


Figure 1. Our image denoising results in Kodak dataset. Top: Gaussian noise ($\sigma = 25$, $\sigma = 50$), Middle: Poisson noise ($\zeta = 0.01$, 0.05), Bottom: Gamma noise ($k = 100$, 50).

Abstract

Tweedie distributions are a special case of exponential dispersion models, which are often used in classical statistics as distributions for generalized linear models. Here, we reveal that Tweedie distributions also play key roles in modern deep learning era, leading to a distribution independent self-supervised image denoising formula without clean reference images. Specifically, by combining with the recent Noise2Score self-supervised image denoising approach and the saddle point approximation of Tweedie distribution, we can provide a general closed-form denoising formula that can be used for large classes of noise distributions without

ever knowing the underlying noise distribution. Similar to the original Noise2Score, the new approach is composed of two successive steps: score matching using perturbed noisy images, followed by a closed form image denoising formula via distribution-independent Tweedie’s formula. This also suggests a systematic algorithm to estimate the noise model and noise parameters for a given noisy image data set. Through extensive experiments, we demonstrate that the proposed method can accurately estimate noise models and parameters, and provide the state-of-the-art self-supervised image denoising performance in the benchmark dataset and real-world dataset.

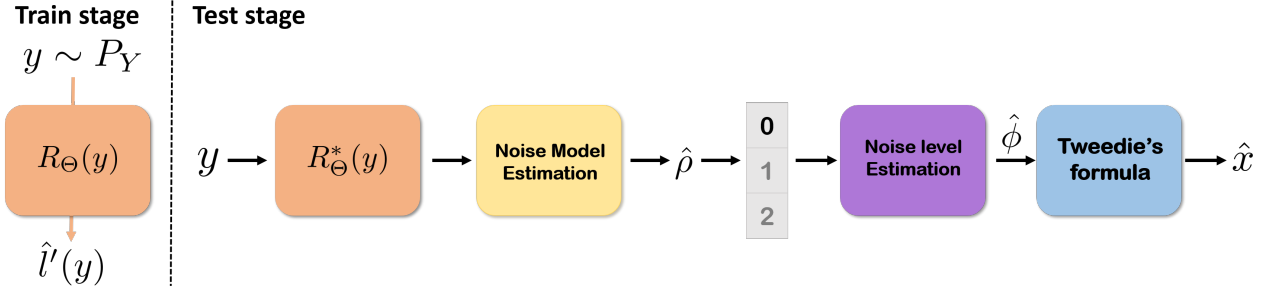


Figure 2. Overall reconstruction flow of the proposed method, where the first step is the estimation of the score function \hat{l}' by training a neural network R_{Θ} , which is followed by the estimation of noise model and noise level to obtain final denoised results. During the training procedure, input images y that belong to the distribution of train set P_Y , are sampled.

1. Introduction

Image denoising is a fundamental problem in low-level vision problems. Nowadays, typical supervised learning approaches easily outperform classical denoising algorithms such as Block-Matching and 3D filtering (BM3D) [2] and Weighted Nuclear Norm Minimization (WNNM) [5]. Nonetheless, the supervised approaches are not practical in many real-world applications as they require a large number of matched clean images for training.

To address this issue, researchers have proposed various forms of self-supervised learning approaches trained with ingenious forms of loss functions that are not associated with clean reference images [1, 6, 9, 12, 14, 21]. Specifically, these approaches have focused on designing loss functions to prevent from learning identity mapping, and can be categorized into two classes: 1) one with generating altered target images from noisy input images [1, 6, 12, 14], and 2) the other by adding regularization terms from Stein’s Unbiased Risk Estimation (SURE) [9, 21].

Although these algorithms appear seemingly different, a recent proposal of Noise2Score [10] revealed that the procedure of generating altered target images or SURE-based regularization term is closely related to the score matching [7], and there exists a minimum mean square error (MMSE) optimal denoising formula in terms of score function for any exponential family distributions. Unfortunately, in the case of truly blind image denoising problem where noise statistics are unknown, Noise2Score cannot provide an optimal performance.

One of the most important contributions of this paper is, therefore, the discovery that the classic Tweedie distribution can provide a “magic” recipe that can be used for a large class of noise distribution even without knowing the distribution. Specifically, Tweedie distribution can be synergistically combined with Noise2Score to provide an explicit de-noising formulation and an algorithm for estimating the underlying noise distributions and parameters. In particular, inspired by the fact that various exponential family distribu-

tions like Gaussian, Gamma, Poisson, etc. can be described by saddle point approximation of the Tweedie distribution by simply changing one parameter, we provide a universal noise removal formula that can be used for a large class exponential family distributions without prior knowledge of the noise model. Furthermore, by assuming that slightly perturbed noisy image may produce similar denoising results, we provide a systematic algorithm that can estimate the noise type and associate parameters for any given images.

In spite of the blind nature of the algorithm, experimental results demonstrated that our method outperforms other self-supervised image denoising methods that are trained with prior knowledge of noise distributions. Our contribution can be summarized as follows.

- We provide a general closed-form denoising formula for large classes of noise distributions by combining Noise2Score approach and the saddle point approximation of Tweedie distribution.
- We propose an algorithm to estimate the noise model and noise parameter for given noisy images. In particular, the proposed noise estimation algorithm significantly improves the performance and boosts the inference speed compared to the original Noise2Score [10].
- We show that the proposed method results in the state-of-the-art performance amongst various self-supervised image denoising algorithms in the benchmark dataset and real-environment dataset.

2. Related Works

2.1. Self-supervised image denoising

Recently, self-supervised image denoising methods using only noisy images have been widely explored. Noise2Noise [14] (N2N) was proposed to train a neural network by minimizing L_2 distance between the noisy image and another noisy realization of the same source im-

age. When additional noisy versions of the same image are not available, Noise2Void (N2V) [12], Noise2Self (N2S) [1] adopted the blind spot network to avoid learning the identity noisy images. Other types of mask-based blind-spot network methods have been explored, which include Self2Self [20], Noise2Same [25], Laine19 [13], etc. Instead of using blind-spot methods, Neighbor2Neighbor (Nei2Nei) [6] generate training image pairs by using the random neighbor sub-sampler method. Noisier2Noise [18] samples doubly noisy images by adding synthetic noises on the single noisy input. Additionally, Soltanayev et al [21] proposed a training scheme using Stein’s unbiased risk estimator (SURE) to denoise additive Gaussian noise. By extending this idea, in [9], the authors proposed a loss function using Poisson Unbiased risk estimator (PURE) to train deep neural network for Poisson noises.

However, these methods have been mostly designed either by distribution independent heuristics, or for specific noise models and we are not aware of any general methods that can be used for a large class of noise distributions by estimating the noise model and parameters.

2.2. Noise2Score

Recently, Noise2Score [10] was proposed to estimate clean images by Tweedie’s formula given the learned score function of noisy data. Specifically, Noise2Score [10] consists of two steps: score function estimation using noisy images, which is followed by Tweedie’s formula to estimate the clean images. To learn the score function from noisy data y , Noise2Score employes the amortized residual DAE (AR-DAE) [15], which is a stabilized implementation of denoising autoencoder (DAE) [24]. In fact, this procedure is closely related to the masking procedure in Noise2Void, Noise2Self, Noiser2Noise, etc.

Once the score function $l'(y)$ for the noisy image is learned, Noise2Score provides an explicit formula for the clean image using Tweedie’s formula. More specifically, consider an exponential family of probability distributions:

$$p(y|\eta) = p_0(y) \exp(\eta^\top T(y) - A(\eta)) \quad (1)$$

where the superscript \top denotes the transpose operation. Here, η is a canonical (vector) parameter of the family, $T(y)$ is a (vector) function of y , $A(\eta)$ is the cumulant generating function which makes $p(y|\eta)$ integrate to 1, and $p_0(y)$ the density up to a scale factor when $\eta = 0$. Then, Tweedie’s formula [4] shows that the posterior estimate of the canonical parameter $\hat{\eta}$ should satisfy the following equation:

$$\hat{\eta}^\top T'(y) = -l'_0(y) + l'(y) \quad (2)$$

where $l'(y) := \nabla_y \log p(y)$ and $l'_0(y) := \nabla_y \log p_0(y)$ are score functions, and $T'(y) = \nabla_y T(y)$ [10].

3. Main Contribution

In practice, when noisy images are collected, it is difficult to assume the underlying noise models. For example, low dose X-ray CT images are contaminated with a lot of noises, but it is not clear whether it is from Gaussian noise, Poisson noises, or mixed distribution. Usually, a specific noise model is assumed for noise removal, but when the assumed noise model is incorrect, there exists an unavoidable bias in the estimated images. The situation is same in Noise2Score, as a specific form of Tweedie’s formula is used depending on the assumed noise model. Therefore, a fundamental question for image denoising is whether there is a universal algorithm that can be used for various noise models without losing its optimality.

In this section, we answer this question affirmatively. Specifically, we show that the classical Tweedie distribution model is a versatile tool that can be combined with Noise2Score to provide a near optimal solution for various noise distribution without even knowing the underlying noise model.

3.1. Tweedie distribution

The Tweedie distributions are a family of probability distributions which include the purely continuous normal, gamma and Inverse Gaussian distributions, the purely discrete scaled Poisson distribution, and the class of compound Poisson–gamma distributions [8]. Specifically, for a random variable y which follows an exponential dispersion model, the Tweedie density function is given by

$$p(y; \mu, \phi) = b_\rho(y, \phi) \exp\left(\frac{-d(y, \mu)}{2\phi}\right), \quad (3)$$

where μ is the mean, $\phi > 0$ is the dispersion parameter which is related to noise level, $d(y, \mu)$ is the unit deviance for $\rho \neq 0, 1, 2$:

$$d(y, \mu) = 2 \left(\frac{y^{2-\rho}}{(1-\rho)(2-\rho)} - \frac{y\mu^{1-\rho}}{1-\rho} + \frac{\mu^{2-\rho}}{2-\rho} \right). \quad (4)$$

Tweedie family densities are characterized by power variance functions of the form $V[\mu] = \phi\mu^\rho$, where $\rho \in (-\infty, 0] \cup [1, \infty)$ is the index determining the distribution [8]. This has a closed form expression for special cases, such as the normal distribution ($\rho = 0$), Poisson ($\rho = 1$), gamma ($\rho = 2$) and inverse Gaussian ($\rho = 3$) distributions (see Table 1). However, the function $b_\rho(y, \phi)$ cannot be written in closed form except for special cases.

Thus, the saddle point approximation can be often used to approximate the Tweedie densities, where $b_\rho(y, \phi)$ is replaced by a simple analytic expression, which leads to a simple expression of the density [3]:

$$p(y; \mu, \phi) = (2\pi\phi y^\rho)^{-\frac{1}{2}} \exp\left(\frac{-d(y, \mu)}{2\phi}\right). \quad (5)$$

Table 1. Exponential dispersion models with power variance functions.

Distribution	ρ	$V[\mu]$	ϕ
Gaussian	0	1	σ^2
Poisson	1	μ	1
Poisson-Gamma	$1 < \rho < 2$	μ^ρ	ϕ
Gamma(α, β)	2	μ^2	$1/\alpha$
Inverse Gaussian	3	μ^3	ϕ

In the following section, we show that (14) is the key to derive a universal denoising formula that can be used for various forms of Tweedie distribution.

3.2. Noise2Score for Tweedie distribution

Now using the same idea of Noise2Score that relies on (13), we can obtain the following universal denoising formula from the saddle point approximation (14). All the proofs in this section are deferred to Supplementary Material.

Proposition 1. For the given measurement model (14), the MMSE optimal estimate of the unknown μ is given by

$$\hat{\mu} = \mathbb{E}[\mu|y] = y(1 + (1 - \rho)\alpha(y, \rho, \phi))^{\frac{1}{1-\rho}} \quad (6)$$

where

$$\alpha(y, \rho, \phi) = \phi y^{\rho-1} \left(\frac{\rho}{2y} + l'(y) \right).$$

Proposition 2. The estimate (6) converges to the specific formulae in Table 2 for given parameter pairs (ρ, ϕ) .

Table 2. Special cases of Tweedie’s formula for denoising.

Distribution	ρ	ϕ	$\hat{\mu}$
Gaussian	0	σ^2	$y + \sigma^2 l'(y)$
Poisson	1	ζ	$\left(y + \frac{\zeta}{2}\right) \exp(\zeta l'(y))$
Gamma(α, α)	2	$1/\alpha$	$\frac{\alpha y}{(\alpha-1) - y l'(y)}$

Note that the specific formula in Table 2 is equivalent to that of the original paper of Noise2Score [10]. This suggests that by simply estimating the parameter pair (ρ, ϕ) , we can estimate both noise model via ρ and noise levels with ϕ . In the following, we provide a systematic algorithm to estimate these parameters from a given noisy measurement.

3.3. Noise Model and Level Estimation

3.3.1 Noise model estimation

Here, we provide an algorithm that can be used to estimate the noise model parameter ρ . Let y_1 be the noisy measurement. Suppose we add a small amount of independent noise

to generate y_1 :

$$y_2 = y_1 + \epsilon u, \quad u \sim \mathcal{N}(0, I)$$

where ϵ is a small known value. If the injected noises are sufficiently small, one could expect that their denoised images using (6) should be similar, i.e.

$$\mathbb{E}[\mu | y_1] \simeq \mathbb{E}[\mu | y_2] \quad (7)$$

Therefore, we have $\alpha(y_1, \rho, \phi) \simeq \alpha(y_2, \rho, \phi)$, which is equivalent to:

$$\phi y_1^{\rho-1} \left(\frac{\rho}{2y_1} + l'(y_1) \right) \simeq \phi y_2^{\rho-1} \left(\frac{\rho}{2y_2} + l'(y_2) \right) \quad (8)$$

Now, the key observation is that the noise level parameter ϕ can be canceled from (25) when the equality holds. Therefore, (25) provides a closed form formula for the noise model parameter ρ as stated in the following proposition.

Proposition 3. Suppose that equality holds in (25) for $y_1 \neq y_2$. Then, the distribution parameter ρ is given by

$$\hat{\rho} = \frac{-a(b-2) \pm \sqrt{(a(b-2))^2 - 4a(-2ab+w)}}{2a} \quad (9)$$

where $a = \log(\frac{y_2}{y_1})$, $b = 2y_1 l'(y_1)$ and $w = 2y_2 l'(y_2) - 2y_1 l'(y_1)$.

Proposition 3 implies that we can estimate the unknown noise model by solving the quadratic equation. Among two solutions for ρ , we empirically determine $\hat{\rho}$ by taking the maximum of two values for the correct estimate of ρ . Since we assume that $\rho \in (0, 2)$, we set the final $\hat{\rho}$ to $\max(0, \hat{\rho})$.

To determine whether underlying noises are either from Gaussian, Poisson, and Gamma, we set the empirical rule to estimate the noise model from $\hat{\rho}$:

$$\begin{cases} \text{Gaussian,} & \text{if } 0 \leq \hat{\rho} < 0.9, \\ \text{Poisson,} & \text{if } 0.9 \leq \hat{\rho} < 1.9, \\ \text{Gamma,} & \text{if } 1.9 \leq \hat{\rho} < 2.9. \end{cases} \quad (10)$$

Specifically, if the estimated model parameter $\hat{\rho}$ is included in a specific range, we conclude that the noisy images belong to corresponding the noise distribution. The detail of implementation are described in Supplementary Material.

3.3.2 Noise level estimation

If the noise model parameter ρ is known or correctly estimated, the universal denoising formula in (6) still require the knowledge of noise level ϕ .

In contrast to the original Noise2Score, which estimates noise level using image quality penalty metric such as total variation (TV), here we propose a novel method to estimate the unknown noise parameter much more efficiently.

Again, the basic intuition is that if the injected noises are sufficiently small, one could expect that their denoised images using (6) should be similar. Proposition 4 provides the specific formula based on the assumption.

Proposition 4. *Assume that the noise model parameter ρ is known. Suppose, furthermore, that the equality holds in (29) for $y_1 \neq y_2$. Then, the noise level parameter of several noise distribution is given by*

$$\begin{cases} \hat{\sigma}^2 = \left(\frac{-\epsilon u}{l'(y_2) - l'(y_1)} \right), & \text{Gaussian,} \\ \hat{\zeta} = \left(-y_1 + \sqrt{y_1^2 - 2c} \right), & \text{Poisson,} \\ \hat{\alpha} = \hat{\beta} = \hat{k} = \left(1 + \frac{l'(y_2) - l'(y_1)}{\frac{1}{y_2} - \frac{1}{y_1}} \right), & \text{Gamma,} \end{cases} \quad (11)$$

where $c = \epsilon u / (l'(y_2) - l'(y_1))$.

For the case of Poisson noise, the solution is derived from the quadratic equation for ζ . Due to $\zeta > 0$, we only calculate the solution with a positive sign. All these formulae are applied for each pixel level, so we should use the median for the pixel level estimate.

In contrast to Noise2Score which requires multiple inferences for the noise level estimation, our proposed method requires only one more inference step to find unknown noise level parameter. Thus, the proposed method has advantages in terms of speed and simplicity.

4. Experimental Results

4.1. Implementation Details

Training Details In order to fairly compare the proposed method with other comparison methods, a modified version of U-Net generator [12] is used for all methods. The mini-batch size was adopted as 16 and the total epoch was set to 100 for training. The Adam optimizer [11] was used to train the neural network with an initial learning rate 2×10^{-4} . The learning rate was decayed to 2×10^{-5} after 50 epochs. To train the score model in this work, we employed the AR-DAE in Noise2Score method [10] and adopt the exponential moving average method with decay rate 0.999. For the annealing sigma σ_a which is required to learn the score function of noisy data, we generate geometric sequences which have the value of the perturbed noise level from σ_a^{max} to σ_a^{min} [22]. Further details of implementation are described in Supplementary Material. Our method was implemented in PyTorch [19] with NVIDIA GeForce GTX 2080-Ti.

Datasets for Synthetic Experiments We used DIV2K [23] and CBSD400 [16] dataset as training data set. We sampled 220,000 cropped patches of 128×128 size to train the network. For the data augmentation, we used the random horizontal, vertical flip, and flop methods.

We generated the synthetic noise images for blind noise cases where noise levels are randomly sampled from the particular range for each noise distribution. In the case of Gaussian noise, noise levels varied with $\sigma \in [5, 55]$. For Poisson noise, noise levels varied with $\zeta \in [0.1, 0.005]$. For Gamma noise, noise levels are in $k \in [40, 120]$. To evaluate the proposed method for blind synthetic noise experiment, the test set was adopted for Kodak, CBSD68 [16] dataset.

4.2. Results of Synthetic Experiments.

Gaussian noise To evaluate our method on various noise distribution, we adopted the nine comparison methods such as BM3D [2], N2V [12], N2S [1], Nei2Nei [6], Laine19 [13], N2Score [10], N2N [14], and supervised learning approaches as shown in Table 3. Comparison methods are varied depending on the noise distribution. The supervised learning and N2N using multiple pair images perform best, but are not practical. In the case of additive Gaussian noise, our method not only outperforms the other self-supervised learning approaches for all of dataset but also provides comparable results to the supervised learning approaches. Thanks to the improved score function estimation described in Supplementary Material, our method provides even better performance of N2Score. The qualitative comparison in Figs. 3 and 4 show that the proposed method provides the best reconstruction results.

Poisson noise For the Poisson noise case, BM3D was replaced with Anscombe transformation (BM3D+VST) as indicated in Table 3. Our proposed method provides significant gain in performance compared to other algorithms, although Laine19-pme, taking advantage of the noise model with known prior, shows the best performance for the Poisson case. Note that our proposed method assumes that the noise model is unknown and estimates the noise statistics. Despite the unknown noise model, the results of proposed method are still comparable. We found that our method significantly improved the results of Noise2Score in Poisson case when the noise level parameter is unknown. It confirmed that the proposed noise level estimation method is more effective than quality penalty metrics in Noise2Score. The visual comparison results in Figs. 3 and 4 show that our method delivers much visually pleasing results compared to other self-supervised methods.

Gamma noise As the extension of BM3D and Laine19 for Gamma noises are not available, we only used six comparison methods to evaluate the proposed method, as indicated in Table 3. In the case of Gamma noise case, we set $\alpha = \beta = k$. Again, the proposed method yields the best results against self-supervised learning approaches and significantly improves the performance of Noise2Score with a margin of ~ 1 dB. The qualitative comparison in Figs. 3 and 4 confirm that our method provides competitive visual

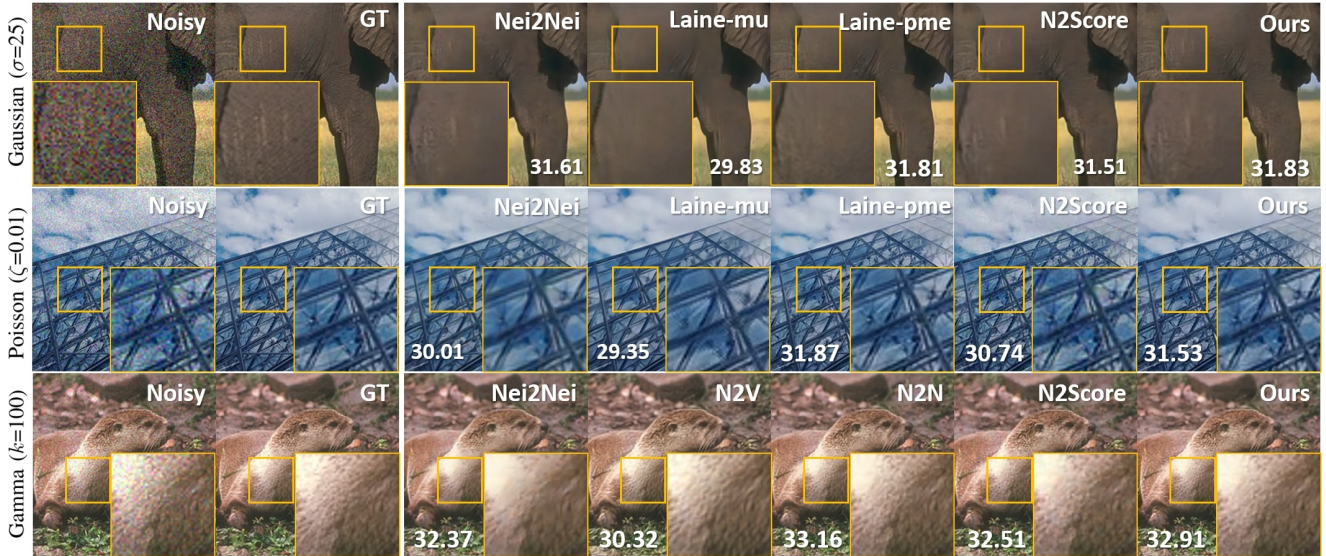


Figure 3. Visual comparison of our method against other competing methods in CBS68 dataset. Top : Gaussian noise with $\sigma = 25$. Middle: Poisson noise with $\zeta = 0.01$. Bottom: Gamma noise with $k = 100$. The number at the lower corner of images indicates the PSNR value in dB.

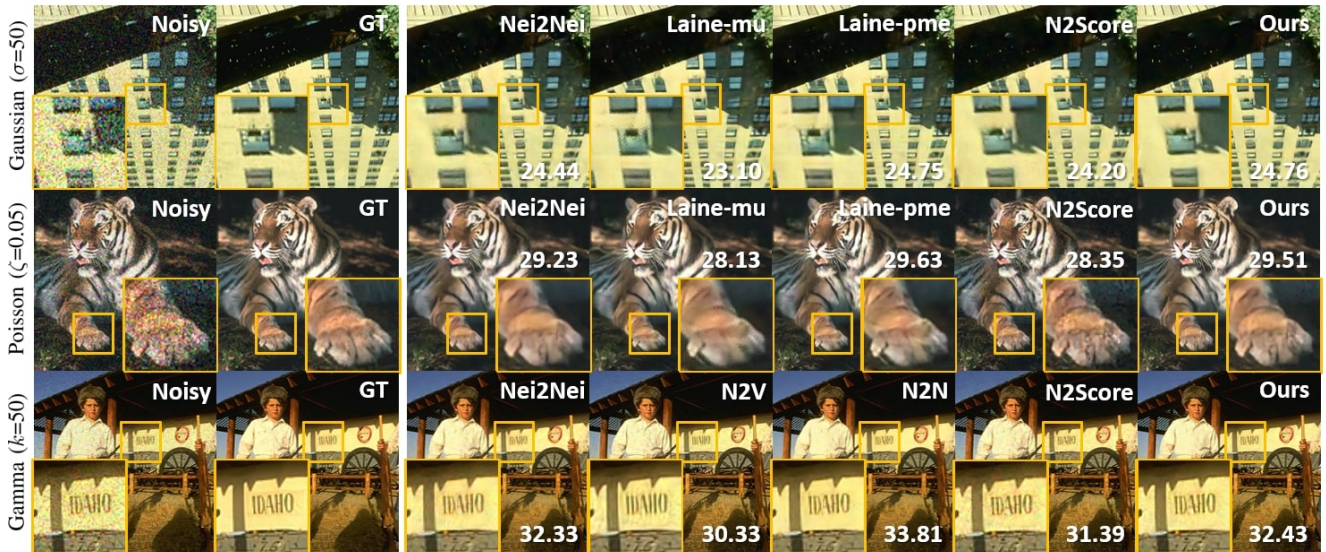


Figure 4. Visual comparison of our method against other competing methods in CBS68 dataset. Top : Gaussian noise with $\sigma = 50$. Middle: Poisson noise with $\zeta = 0.05$. Bottom: Gamma noise with $k = 50$. The number at the lower corner of the image indicates the PSNR value in dB.

quality among self-supervised deep denoisers.

4.3. Real Image Noise Removal

To verify that the algorithm can be applied to a real dataset, a real noise removal experiment was performed using the AAPM CT dataset [17], which contains 4358 images in 512×512 resolution from 10 different patients at low-

dose level and high-dose X-ray levels. The input images are adopted as quarter dose images and the target images are set to full dose images. We randomly select 3937 images as a train set, and the remaining 421 images are set as a test set. The noise distribution in X-ray photon measurement and in the sinogram are often modeled as Poisson noise and Gaussian noise, but real noise in reconstructed images is spatially

Table 3. Quantitative comparison of denoising results by various methods in terms of PSNR(dB) when the noise parameters are unknown (N2V: Noise2Void, N2S: Noise2Self, Nei2Nei: Neighbor2Neighbor, N2Score: Noise2Score, N2N: Noise2Noise, SL: supervised learning, Anscombe: Anscombe method for BM3D).

Noise type		Conventional	Self-Supervised							Supervised	
Gaussian	Dataset	BM3D	N2V	N2S	Nei2Nei	Laine19-mu	Lain19-pme	N2Score	Ours	N2N	SL
$\sigma = 25$	CBSD68	28.61	29.22	29.71	30.56	28.61	30.88	30.75	30.89	30.92	30.92
	Kodak	29.94	30.02	30.81	31.55	30.19	31.92	31.78	31.95	31.96	31.96
$\sigma = 50$	CBSD68	26.71	25.13	27.14	27.32	26.42	27.65	27.32	27.56	27.73	27.73
	Kodak	27.02	25.75	28.21	28.28	27.78	28.63	28.23	28.64	28.70	28.71
Poisson	Dataset	Anscombe	N2V	N2S	Nei2Nei	Laine19-mu	Lain19-pme	N2Score	Ours	N2N	SL
$\zeta = 0.01$	CBSD68	30.68	31.02	30.74	31.64	30.61	32.73	31.87	32.53	32.94	32.95
	Kodak	31.93	31.98	31.92	32.61	31.67	33.51	32.96	33.41	33.86	33.87
$\zeta = 0.05$	CBSD68	26.93	28.12	28.33	28.46	27.53	28.83	28.27	28.73	29.07	29.07
	Kodak	28.27	29.32	29.49	29.54	28.68	30.17	28.98	29.72	30.23	30.25
Gamma	Dataset		N2V	N2S	Nei2Nei			N2Score	Ours	N2N	SL
$k = 100$	CBSD68	-	31.83	31.71	34.21	-	-	33.82	34.52	35.33	35.33
	Kodak	-	31.66	32.83	35.10	-	-	34.23	35.42	36.16	36.16
$k = 50$	CBSD68	-	30.51	30.63	32.11	-	-	31.32	32.43	33.41	33.41
	Kodak	-	31.38	31.71	32.38	-	-	31.81	32.81	34.39	34.40

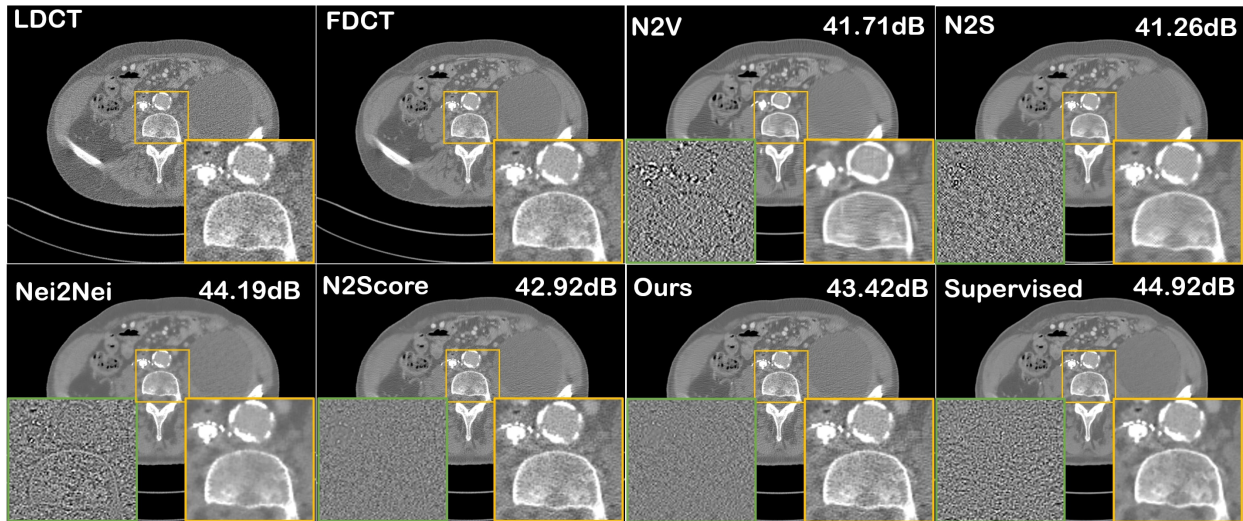


Figure 5. Denoising results of AAPM data using various methods. The yellow box and green box show the enlarged view of image and difference image between network input and output, respectively. The intensity window of CT image is $(-500,500)$ [HU] and the intensity window of difference is $(-200,200)$ [HU].

correlated and more complicated, so that it leads to difficulties in modeling the specific noise distributions.

To deal with blind image noise removal in the low dose CT images, we carried out experiment with the proposed method using the procedure in Fig. 2. The other experiment settings are identical to synthetic experiments. Based on the model estimation rule in (10), we observed that the Low-dose CT images can be interpreted as corrupted by Gaussian noise ($\hat{\rho} \simeq 0$). To evaluate the proposed method, we compare with other methods such as N2S [1], N2V [12],

Nei2Nei [6], N2Score [10], and supervised learning approach. To implement the original Noise2Score, we assume that the noise distribution is additive Gaussian noise. The quantitative results suggest that the proposed method yields the competitive results to other self-supervised learning approaches. However, the visual quality is also an important criterion to evaluate the results in the medical imaging. In Fig 8, the qualitative comparison shows that other self-supervised approaches provide over-smooth denoised images. In particular, the difference images of these meth-

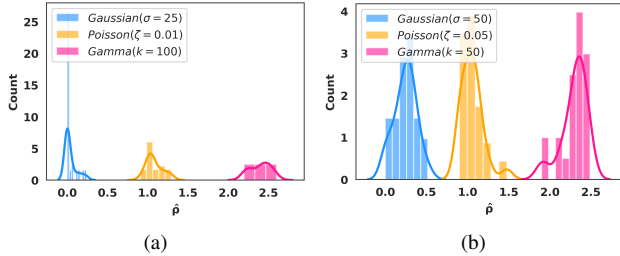


Figure 6. The histogram of estimated noise model parameter $\hat{\rho}$ in Kodak dataset. (a) For the case of $\sigma = 25$, $\zeta = 0.01$, $k = 100$. (b) For the case of $\sigma = 50$, $\zeta = 0.05$, $k = 50$.

ods show the structure of CT images. However, our method yields visually similar results compared to full-dose CT image and also provides only noises in the difference image between the network input and output. Therefore, our method also has the advantage that it can be applied to real environment dataset.

Table 4. Quantitative comparison using various methods in terms of PNSR(dB) on the AAPM CT dataset. (N2V: Noise2Void, N2S: Noise2Self, Nei2Nei: Neighbor2Neighbor, N2Score: Noise2Score SL: supervised learning).

Method	N2S	N2V	Nei2Nei	N2Score	Ours	SL
PNSR	35.82	35.93	37.83	36.63	36.92	38.53

5. Ablation Study

5.1. Results on Noise model estimation

Here, we validate the proposed the noise model estimation by (10). Figure 6 shows the histogram of estimated noise model parameter $\hat{\rho}$ in the Kodak dataset. We have calculated $\hat{\rho}$ for each noise distribution and plot distributions in each figure. According to Tweedie’s distribution, we expect that the parameters of noise model can be differentiated for each noise distribution such as Gaussian ($\hat{\rho} \simeq 0$), Poisson ($\hat{\rho} \simeq 1$), and Gamma ($\hat{\rho} \simeq 2$). From the figure, we can observe that the noise model parameters $\hat{\rho}$ are distinctly distributed in the case of low noise levels. Furthermore, in the case of high noise levels, the distributions can also be distinguished for each noise distribution. It implies that it was possible to successfully estimate the noise model with the proposed method, so that it leads to the use of the exact Tweedie’s formula for blind image denoising.

Table 5. Reconstruction results with various noise parameter estimation methods on CBSD68 dataset in terms of PSNR(dB).

Noise type	Quality Penalty	Ours	Known value	SL
Gaussian ($\sigma=25$)	30.78	30.89	30.91	30.92
Poisson ($\zeta=0.01$)	31.89	32.53	32.63	32.95
Gamma ($k=100$)	33.92	34.52	34.53	35.33
Inference speed	3.1s	0.1s	-	-

5.2. Ablation study on Noise level estimation

We analyze the effect of the proposed noise level estimation by comparing quality penalty metric [10] and others. To fairly evaluate the proposed method, we used an identical weights of the score model for each case. We carried out an ablation study by fixing the noise model estimation procedure and by only varying the noise level estimation as shown Table 6. Here, “known value” refers to the results assuming the known ground truth noise level parameter. “SL” denotes that the results of supervised learning. We found that quality penalty metric yield comparable performance to “known value” in the case of the Gaussian, but the performance with the quality penalty metric decreased for the case of Poisson and Gamma noises. However, the proposed methods outperform the quality penalty metric approach and yields results comparable to “known value” in all cases. Furthermore, we compare the inference speed of the estimation stage. The quality penalty metric method took about $\times 30$ times more to estimate noise level parameters compared to our method.

6. Conclusion

In this article, we provided a novel self-supervised blind image denoising framework that does not require clean data and prior knowledge of noise models and levels. Our innovation came from the saddle point approximation of Tweedie distributions, which cover a wide range of exponential family distributions. By taking advantage of this property, we provided a universal denoising formula that can be used for various distributions in real life. Furthermore, we proposed a novel algorithm that can estimate the noise model and noise level parameter in a unified framework. Finally, we validated the proposed method using benchmark and real CT image data sets, and confirmed that the method outperforms the existing state-of-the-art self-supervised learning methods.

References

- [1] Joshua Batson and Loic Royer. Noise2Self: Blind denoising by self-supervision. In *International Conference on Machine Learning*, pages 524–533. PMLR, 2019. [2](#), [3](#), [5](#), [7](#)
- [2] Kostadin Dabov, Alessandro Foi, Vladimir Katkovnik, and Karen Egiazarian. Image denoising with block-matching and 3D filtering. In *Image Processing: Algorithms and Systems, Neural Networks, and Machine Learning*, volume 6064, page 606414. International Society for Optics and Photonics, 2006. [2](#), [5](#)
- [3] Peter K Dunn and Gordon K Smyth. Tweedie family densities: methods of evaluation. In *Proceedings of the 16th international workshop on statistical mod-*

- elling, Odense, Denmark, pages 2–6. Citeseer, 2001. 3, 10
- [4] Bradley Efron. Tweedie’s formula and selection bias. *Journal of the American Statistical Association*, 106(496):1602–1614, 2011. 3, 10
- [5] Shuhang Gu, Lei Zhang, Wangmeng Zuo, and Xiangchu Feng. Weighted nuclear norm minimization with application to image denoising. In *Proceedings of the IEEE conference on computer vision and pattern recognition*, pages 2862–2869, 2014. 2
- [6] Tao Huang, Songjiang Li, Xu Jia, Huchuan Lu, and Jianzhuang Liu. Neighbor2neighbor: Self-supervised denoising from single noisy images. In *Proceedings of the IEEE/CVF Conference on Computer Vision and Pattern Recognition*, pages 14781–14790, 2021. 2, 3, 5, 7
- [7] Aapo Hyvärinen and Peter Dayan. Estimation of non-normalized statistical models by score matching. *Journal of Machine Learning Research*, 6(4), 2005. 2
- [8] Bent Jørgensen. *The theory of dispersion models*. CRC Press, 1997. 3
- [9] Kwanyoung Kim, Shakarim Soltanayev, and Se Young Chun. Unsupervised Training of Denoisers for Low-Dose CT Reconstruction Without Full-Dose Ground Truth. *IEEE Journal of Selected Topics in Signal Processing*, 14(6):1112–1125, 2020. 2, 3
- [10] Kwanyoung Kim and Jong Chul Ye. Noise2score: Tweedie’s approach to self-supervised image denoising without clean images. *arXiv preprint arXiv:2106.07009*, 2021. 2, 3, 4, 5, 7, 8, 10, 12, 13, 14
- [11] Diederik P Kingma and Jimmy Ba. Adam: A method for stochastic optimization. *arXiv preprint arXiv:1412.6980*, 2014. 5
- [12] Alexander Krull, Tim-Oliver Buchholz, and Florian Jug. Noise2Void-learning denoising from single noisy images. In *Proceedings of the IEEE/CVF Conference on Computer Vision and Pattern Recognition*, pages 2129–2137, 2019. 2, 3, 5, 7
- [13] Samuli Laine, Tero Karras, Jaakko Lehtinen, and Timo Aila. High-quality self-supervised deep image denoising. *arXiv preprint arXiv:1901.10277*, 2019. 3, 5
- [14] Jaakko Lehtinen, Jacob Munkberg, Jon Hasselgren, Samuli Laine, Tero Karras, Miika Aittala, and Timo Aila. Noise2Noise: Learning image restoration without clean data. *arXiv preprint arXiv:1803.04189*, 2018. 2, 5
- [15] Jae Hyun Lim, Aaron Courville, Christopher Pal, and Chin-Wei Huang. AR-DAE: Towards Unbiased Neural Entropy Gradient Estimation. In *International Conference on Machine Learning*, pages 6061–6071. PMLR, 2020. 3
- [16] David Martin, Charless Fowlkes, Doron Tal, and Jitendra Malik. A database of human segmented natural images and its application to evaluating segmentation algorithms and measuring ecological statistics. In *Proceedings Eighth IEEE International Conference on Computer Vision. ICCV 2001*, volume 2, pages 416–423. IEEE, 2001. 5
- [17] Cynthia H McCollough, Adam C Bartley, Rickey E Carter, Baiyu Chen, Tammy A Drees, Phillip Edwards, David R Holmes III, Alice E Huang, Farhana Khan, Shuai Leng, et al. Low-dose ct for the detection and classification of metastatic liver lesions: results of the 2016 low dose ct grand challenge. *Medical physics*, 44(10):e339–e352, 2017. 6, 14
- [18] Nick Moran, Dan Schmidt, Yu Zhong, and Patrick Coady. Noisier2noise: Learning to denoise from unpaired noisy data. In *Proceedings of the IEEE/CVF Conference on Computer Vision and Pattern Recognition*, pages 12064–12072, 2020. 3
- [19] Adam Paszke, Sam Gross, Soumith Chintala, Gregory Chanan, Edward Yang, Zachary DeVito, Zeming Lin, Alban Desmaison, Luca Antiga, and Adam Lerer. Automatic differentiation in pytorch. 2017. 5, 13
- [20] Yuhui Quan, Mingqin Chen, Tongyao Pang, and Hui Ji. Self2self with dropout: Learning self-supervised denoising from single image. In *Proceedings of the IEEE/CVF Conference on Computer Vision and Pattern Recognition*, pages 1890–1898, 2020. 3
- [21] Shakarim Soltanayev and Se Young Chun. Training and Refining Deep Learning Based Denoisers without Ground Truth Data. *arXiv preprint arXiv:1803.01314*, 2018. 2, 3
- [22] Yang Song and Stefano Ermon. Improved techniques for training score-based generative models. *arXiv preprint arXiv:2006.09011*, 2020. 5, 12
- [23] Radu Timofte, Shuhang Gu, Jiqing Wu, Luc Van Gool, Lei Zhang, Ming-Hsuan Yang, Muhammad Haris, et al. NTIRE 2018 challenge on Single Image Super-Resolution: Methods and Results. In *The IEEE Conference on Computer Vision and Pattern Recognition (CVPR) Workshops*, June 2018. 5
- [24] Pascal Vincent, Hugo Larochelle, Isabelle Lajoie, Yoshua Bengio, Pierre-Antoine Manzagol, and Léon Bottou. Stacked denoising autoencoders: Learning useful representations in a deep network with a local denoising criterion. *Journal of machine learning research*, 11(12), 2010. 3

[25] Yaochen Xie, Zhengyang Wang, and Shuiwang Ji. Noise2Same: Optimizing a self-supervised bound for image denoising. *arXiv preprint arXiv:2010.11971*, 2020. 3

Appendix

A. Proof of Proposition 1

Proof. For a given exponential family of probability distributions:

$$p(y|\mu) = p_0(y) \exp(\mu^\top T(y) - A(\mu)), \quad (12)$$

Tweedie's formula [4] shows that the posterior estimate of the canonical parameter $\hat{\mu}$ should satisfy the following equation:

$$\hat{\mu}^\top T'(y) = -l'_0(y) + l'(y) \quad (13)$$

where $l'(y) := \nabla_y \log p(y)$ and $l'_0(y) := \nabla_y \log p_0(y)$ are score functions, and $T'(y) = \nabla_y T(y)$ [10].

Now, our goal is to use this formula to the saddle point approximation of Tweedie distribution [3] given by:

$$p(y; \mu, \phi) = (2\pi\phi y^\rho)^{-\frac{1}{2}} \exp\left(\frac{-d(y, \mu)}{2\phi}\right) \quad (14)$$

where

$$d(y, \mu) = 2 \left(\frac{y^{2-\rho}}{(1-\rho)(2-\rho)} - \frac{y\mu^{1-\rho}}{1-\rho} + \frac{\mu^{2-\rho}}{2-\rho} \right). \quad (15)$$

By inspection of (12) and (14), we have

$$\begin{aligned} p_0(y) &= (2\pi\phi y^\rho)^{-\frac{1}{2}} \\ \mu^\top T(y) - A(\mu) &= \frac{-d(y, \hat{\mu})}{2\phi} \end{aligned} \quad (16)$$

Furthermore, we have

$$\begin{aligned} \frac{\partial d(y, \mu)}{\partial y} &= \frac{2}{1-\rho} y^{1-\rho} - \frac{2}{1-\rho} \mu^{1-\rho} \\ \frac{\partial \log(2\pi\phi y^\rho)^{-\frac{1}{2}}}{\partial y} &= -\frac{\rho}{2y} \end{aligned}$$

Accordingly,

$$\begin{aligned} \hat{\mu}^\top T'(y) &= -\frac{1}{\phi(1-\rho)} (y^{1-\rho} - \hat{\mu}^{1-\rho}) \\ &= \frac{\rho}{2y} + l'(y) \end{aligned}$$

which leads to

$$\hat{\mu}^{1-\rho} = y^{1-\rho} + \phi(1-\rho) \left(\frac{\rho}{2y} + l'(y) \right). \quad (17)$$

Therefore, we have

$$\begin{aligned} \hat{\mu} &= \exp \left\{ \frac{1}{1-\rho} \log \left(y^{1-\rho} + \phi(1-\rho) \left(\frac{\rho}{2y} + l'(y) \right) \right) \right\} \\ &= y(1 + (1-\rho)\alpha(y, \rho, \phi))^{\frac{1}{1-\rho}} \end{aligned} \quad (18)$$

where

$$\alpha(y, \rho, \phi) = \phi y^{\rho-1} \left(\frac{\rho}{2y} + l'(y) \right). \quad (19)$$

This concludes the proof. \square

B. Proof of Proposition 2

Proof:

Additive Gaussian noise. In this case, we have $\rho = 0$, $\phi = \sigma^2$ for Tweedie distribution. Accordingly, (19) can be simplified as

$$\alpha(y, 0, \phi) = \sigma^2 y^{-1} l'(y) \quad (20)$$

Therefore, using (18), we have

$$\hat{\mu} = y(1 + \sigma^2 y^{-1} l'(y)) = y + \sigma^2 l'(y).$$

Poisson noise. In this case, we have $\rho = 1$, $\phi = \zeta$ for Tweedie distribution. In this case, we have

$$\begin{aligned} &\lim_{\rho \rightarrow 1} (1 + (1-\rho)\alpha(y, \rho, \phi))^{\frac{1}{1-\rho}} \\ &= \exp \left[\lim_{\rho \rightarrow 1} \frac{\log(1 + (1-\rho)\alpha(y, \rho, \phi))}{1-\rho} \right] \\ &= \exp \left[\lim_{\rho \rightarrow 1} \frac{\alpha(y, \rho, \phi)}{1 + (1-\rho)\alpha(y, \rho, \phi)} \right] \\ &= \exp[\alpha(y, 1, \phi)]. \end{aligned} \quad (21)$$

where the second equality comes from the L'Hospital's rule, and

$$\alpha(y, 1, \phi) = \zeta \left(\frac{1}{2y} + l'(y) \right) \quad (22)$$

Therefore, we have

$$\begin{aligned} \hat{\mu} &= y \exp \left[\zeta \left(\frac{1}{2y} + l'(y) \right) \right] \\ &= y \exp\left(\frac{\zeta}{2y}\right) \exp(\zeta l'(y)) \\ &\approx \left(y + \frac{\zeta}{2}\right) \exp(\zeta l'(y)), \end{aligned}$$

where the last approximation comes from $\exp(x) \approx 1 + x$ for a small x .

Gamma noise. In this case, we have $\rho = 2, \phi = 1/k$ for Tweedie distribution. Using (19), we have

$$\alpha(y, 2, k) = \frac{1}{k}y \left(\frac{1}{y} + l'(y) \right) = \frac{1}{k}(1 + yl'(y)) \quad (23)$$

Therefore, we have

$$\begin{aligned} \hat{\mu} &= y \left(1 - \frac{1}{k}(1 + yl'(y)) \right)^{-1} \\ &= \frac{ky}{(k-1) - yl'(y)} \end{aligned}$$

This concludes the proof.

C. Proof of Proposition 3

Proof. Let $y_2 = y_1 + \epsilon u$ for $u \sim \mathcal{N}(0, 1)$. Then, we have

$$\alpha(y_1, \rho, \phi) = \phi y_1^{\rho-1} \left(\frac{\rho}{2y_1} + l'(y_1) \right) \quad (24)$$

$$\alpha(y_2, \rho, \phi) = \phi y_2^{\rho-1} \left(\frac{\rho}{2y_2} + l'(y_2) \right) \quad (25)$$

For a sufficiently small perturbation ϵ , we can assume that

$$\alpha(y_1, \rho, \phi) = \alpha(y_2, \rho, \phi)$$

Accordingly, by dividing (25) by (24), we have

$$1 = \left(\frac{y_2}{y_1} \right)^{\rho-1} \left(\frac{\frac{\rho}{2y_2} + l'(y_2)}{\frac{\rho}{2y_1} + l'(y_1)} \right)$$

By taking logarithm on both sides, we have

$$(\rho - 2) \log \left(\frac{y_2}{y_1} \right) + \log \left(\frac{\rho + 2y_2 l'(y_2)}{\rho + 2y_1 l'(y_1)} \right) = 0 \quad (26)$$

Furthermore, by denoting $w := 2y_2 l'(y_2) - 2y_1 l'(y_1)$, we have

$$\begin{aligned} \log \left(\frac{\rho + 2y_2 l'(y_2)}{\rho + 2y_1 l'(y_1)} \right) &= \log \left(1 + \frac{w}{\rho + 2y_1 l'(y_1)} \right) \\ &\approx \frac{w}{\rho + 2y_1 l'(y_1)} \end{aligned} \quad (27)$$

when $\frac{w}{\rho + 2y_1 l'(y_1)} \rightarrow 0$. By plugging (27) into (26), we can obtain the quadratic equation for ρ :

$$0 = (\rho - 2) \log \left(\frac{y_2}{y_1} \right) + \frac{2y_2 l'(y_2) - 2y_1 l'(y_1)}{\rho + 2y_1 l'(y_1)}$$

By denoting $a = \log(\frac{y_2}{y_1}), b = 2y_1 l'(y_1)$, we have

$$\begin{aligned} 0 &= a(\rho - 2) + \frac{w}{\rho + b}, \\ &= a(\rho - 2)(\rho + b) + w. \end{aligned} \quad (28)$$

Therefore, the estimated noise model parameter $\hat{\rho}$ can be obtained as the solutions for the quadratic equation, which is given by:

$$\hat{\rho} = \frac{-a(b-2) \pm \sqrt{(a(b-2))^2 - 4a(-2ab+w)}}{2a}$$

□

D. Proof of Proposition 4

Proof. Let $y_2 = y_1 + \epsilon u$ for $u \sim \mathcal{N}(0, 1)$, and the noise model parameter ρ is known. Suppose furthermore that ϵ is non-zero but sufficiently small that the following equality holds:

$$\mathbb{E}[\mu|y_1] = \mathbb{E}[\mu|y_2] \quad (29)$$

Now, we derive the formula for each distribution.

Additive Gaussian noise For the case of additive Gaussian noise, we have

$$\hat{x}_1 = \mathbb{E}[\mu|y_1] = y_1 + \sigma^2 l'(y_1) \quad (30)$$

$$\hat{x}_2 = \mathbb{E}[\mu|y_2] = y_2 + \sigma^2 l'(y_2) \quad (31)$$

By subtracting (30) from (31), we have

$$-\epsilon u = \sigma^2 (l'(y_2) - l'(y_1)) \quad (32)$$

Thus, we have the following estimate:

$$\hat{\sigma}^2 = \frac{-\epsilon u}{l'(y_2) - l'(y_1)}$$

Poisson noise In this case, we have

$$\hat{x}_1 = \left(y_1 + \frac{\zeta}{2} \right) \exp(\zeta l'(y_1)) \quad (33)$$

$$\hat{x}_2 = \left(y_2 + \frac{\zeta}{2} \right) \exp(\zeta l'(y_2)), \quad (34)$$

By taking the logarithm of both equations and subtracting (33) from (34), we have

$$\begin{aligned} 0 &= \log \left(1 + \frac{\epsilon u}{y_1 + \zeta/2} \right) + \zeta (l'(y_2) - l'(y_1)) \\ &\approx \left(\frac{\epsilon u}{y_1 + \zeta/2} \right) + \zeta (l'(y_2) - l'(y_1)), \end{aligned}$$

where the last approximation comes from $x \approx \log(1+x)$ for sufficiently small x . This leads to the following quadratic equation for ζ :

$$0 = \epsilon u + \zeta (y_1 + \zeta/2) (l'(y_2) - l'(y_1)). \quad (35)$$

Solving quadratic equation (35), we can obtain the following estimate:

$$\hat{\zeta} = y_1 + \sqrt{y_1^2 - 2c}$$

where $c = \epsilon u / (l'(y_2) - l'(y_1))$.

Gamma noise For the case of Gamma noise,

$$\hat{x}_1 = \frac{ky_1}{k-1-y_1l'(y_1)} \quad (36)$$

$$\hat{x}_2 = \frac{ky_2}{k-1-y_2l'(y_2)} \quad (37)$$

By taking the inverse of both equations and subtracting (36) from (37), we have

$$\frac{1}{y_2} - \frac{1}{y_1} = \frac{1}{k} \left(\frac{1}{y_2} - \frac{1}{y_1} + l'(y_2) - l'(y_1) \right).$$

Then, we can obtain \hat{k} by

$$\hat{k} = 1 + \frac{l'(y_2) - l'(y_1)}{\frac{1}{y_2} - \frac{1}{y_1}}$$

□

E. Pseudocode Description

Algorithm 1 details the overall pipeline of the training procedure for the proposed method. First, the neural network R_Θ was trained by minimizing $\ell_{AR-DAE}(\Theta)$ to learn the estimation of the score function from the noisy input y . In the training, noisy images are sampled from an unknown noise model corrupted with various noise levels. This neural network training step is universally applied regardless of noise distribution. In particular, we annealed σ_a from σ_a^{max} to σ_a^{min} to stably train the network as suggested in [22]. Now let Θ' be an independent copy of the parameters and after the n^{th} training iteration, and we update the Θ' with the exponential moving average as indicated in Algorithm 1 as suggested in [22].

The inference of the proposed method is described in Algorithm 2. After we obtain the trained score models $R_{\Theta'}^*$, we firstly estimate the noise model parameter $\hat{\rho}$ with Equation (10) in the main paper using Proposition 3. Once the noise model is determined, we estimate the noise level parameter for the estimated noise model using Proposition 4. Then, the final clean image is reconstructed by Tweedie's formula as indicated in Table 2 in the main paper.

F. Implementation Details

Training details To robustly train the proposed method, we randomly injected the perturbed noise into a noisy image

Algorithm 1: Training procedure of the proposed method

Given: learning rates γ , number of epochs N ;
Input : noisy input y from training data set D_ϕ and noise level parameter $\phi \in (\sigma, \zeta, k)$, neural network R_Θ , independent copy of the parameter Θ' , annealing sigma set S_{σ_a} with size of T , $S_{\sigma_a} = [\sigma_a^{min}, \dots, \sigma_a^{max}]$, decay rate of exponential moving average m

```

1 for  $n = 1$  to  $N$  do
2    $u \sim \mathcal{N}(0, 1)$ ;
3    $t \sim \mathcal{U}(0, T)$ ;
4    $\sigma_a \rightarrow S_{\sigma_a}^t$ ;
5    $\ell_{AR-DAE}(\Theta) = \mathbb{E}_{y \sim P_Y} \|u + \sigma_a R_\Theta(y + \sigma_a u)\|^2$ ;
6    $\Theta \leftarrow \Theta - \gamma \nabla_{\Theta} \ell_{AR-DAE}(\Theta)$ ;
    $\Theta' \leftarrow m\Theta' - (1 - m)\Theta$ ;

```

Output: Trained the score model, $R_{\Theta'}^*(y) = \hat{l}'(y)$

Algorithm 2: Inference procedure of the proposed method

Given: Trained score model $R_{\Theta'}^*$, the perturbed noise level ϵ ;
Input : noisy input y_1 from training data set D_ϕ and noise level parameter $\phi \in (\sigma, \zeta, k)$, and generated perturbed noisy image $y_2 = y_1 + \epsilon\mu$, $\mu \sim \mathcal{N}(0, I)$;
Noise model estimation: $\hat{\rho}$ by Equation (10) in the main paper

Noise level estimation:

```

1 if  $0 \leq \hat{\rho} < 0.9 \rightarrow y \in \text{Gaussian noise}$  then
    $\hat{\sigma}^2 = \text{median} \left( \frac{-\epsilon u}{l'(y_2) - l'(y_1)} \right)$ ;
   Output :  $\hat{x} = y + \hat{\sigma}^2 l'(y_1)$ 
2 else if  $0.9 \leq \hat{\rho} < 1.9 \rightarrow y \in \text{Poisson noise}$  then
    $\hat{\zeta} = \text{median} \left( -y_1 + \sqrt{y_1^2 - 2c} \right)$ ;
   Output :  $\hat{x} = \left( y + \frac{\hat{\zeta}}{2} \right) \exp^{\hat{\zeta} l'(y)}$ 
3 else if  $1.9 \leq \hat{\rho} < 2.9 \rightarrow y \in \text{Gamma noise}$  then
    $\hat{k} = \text{median} \left( 1 + \frac{l'(y_2) - l'(y_1)}{\frac{1}{y_2} - \frac{1}{y_1}} \right)$ ;
   Output :  $\hat{x} = \frac{\hat{k}y}{(\hat{k}-1) - y l'(y)}$ 

```

instead of using linear scheduling as in [10]. In the case of the Gaussian and Gamma noise, σ_a^{max} and σ_a^{min} are set to [0.1, 0.001], respectively. For the Poisson noise case, σ_a^{max} and σ_a^{min} was set to [0.1, 0.02], respectively.

Noise model estimation In order to satisfy the assumption in (27), we only calculate the pixel values that satisfies the following condition:

$$idx = -\epsilon < \frac{w}{\rho + b} < \epsilon \quad (38)$$

where ϵ was set to 1×10^{-5} for all of the cases. In the procedure of calculating (38), we can not access $\hat{\rho}$ value. Hence, based on assumption $\rho \in (0, 2)$, we empirically determine this value. In the case of additive Gaussian noise, this value is set to 2.5, otherwise to 2.2. We provide the implementation code based on Pytorch [19] as shown in Listing 1.

Listing 1. Source code of the proposed noise model estimation

```

1 def noise_model_estimation(y_1, score_model):
2     # Inject noise into noisy images y_1
3     epsilon = 1e-5
4     n = torch.randn(y_1.shape)
5     noise = epsilon * n
6     y_2 = y_1 + noise
7     # estimate the score functions
8     l(y_1) = score_model(y_1)
9     l(y_2) = score_model(y_2)
10    # calculate each coefficient
11    w = 2*(y_2*l(y_2) - y_1*l(y_1))
12    a = torch.log(y_2/y_1)
13    b = (2*y_1*l(y_1))
14    # take only values under condition
15    ww = w/(b+2.2)
16    idx = (ww <= 1e-5) & (ww >= -1e-5)
17    w = w[idx]
18    b = b[idx]
19    w = torch.nanmean(w)
20    b = torch.nanmean(b)
21    # Solve quadratic equation
22    first = a*(b-2)
23    second = 4*a*(- 2*a*b + w)
24    sqrt = (first)**2 - second
25    sqrt = torch.sqrt(sqrt)
26    p1 = (-first + sqrt)/(2*a)
27    p2 = (-first - sqrt)/(2*a)
28    p1 = torch.nanmean(p1)
29    p2 = torch.nanmean(p2)
30    # take maximum of two values
31    p = max(p1,p2)
32    # take maximum of p and 0
33    p = max(p,0)
34    return p

```

Noise level estimation To use Proposition 3, we assume that the injected small noise is sufficiently small, the equality in (29) holds. To achieve this, we set ϵ to 1×10^{-5} for all noise cases.

G. Analysis for Noise Model Estimation

Table 6 shows the accuracy of the estimated noise model in the Kodak dataset. If the estimated noise distributions are equal to the truth noise distributions, we determine that the estimate is correct. We found that the proposed noise model estimation reach 100% accuracy for all cases. Thus, we concluded that we can successfully estimate the noise model with the proposed method.

Table 6. Accuracy of the proposed noise model estimation in the Kodak dataset.

Noise type	Noise level	Accuracy(%)
Gaussian	$\sigma = 25$	100
	$\sigma = 50$	100
Poisson	$\zeta = 0.01$	100
	$\zeta = 0.05$	100
Gamma	$k = 100$	100
	$k = 50$	100

H. Analysis for Noise Level Estimation

Fig. 7 shows the bar graph of estimated noise level parameters for each noise distribution in the Kodak dataset. Similar to the ablation study in the main paper, we carried out the analysis by fixing the noise model estimation and by only varying the estimation of noise level. From the ablation study in the main paper, we expect that the quality penalty metrics method in [10] estimates correctly in the case of additive Gaussian noise, but incorrectly for the case of other noise distributions. We can observe the similar findings in Figure 7. On the other hand, the proposed noise level estimation provides more accurate results compared to the quality penalty metrics in [10] with a small standard deviation. Thus, we can conclude that the proposed noise level estimation can successfully estimate the truth noise level in all noise distribution cases.

I. Ablation Study on Score Estimation

We demonstrate the effectiveness of each component in improving the score model. Table 7 compares the PSNR values of the results with and without each component on CBSD68 dataset (Poisson noise $\zeta = 0.01$). EMA and GS denote Exponential Moving Average and Geometric Sequence, respectively. To fairly compare each case, we performed the ablation study using the same procedure. From the table, we observe the performance degradation when any component of the proposed method is absent. Therefore, we can conclude that EMA and GS in the proposed method are essential for improving the score model in the training procedure of the network.

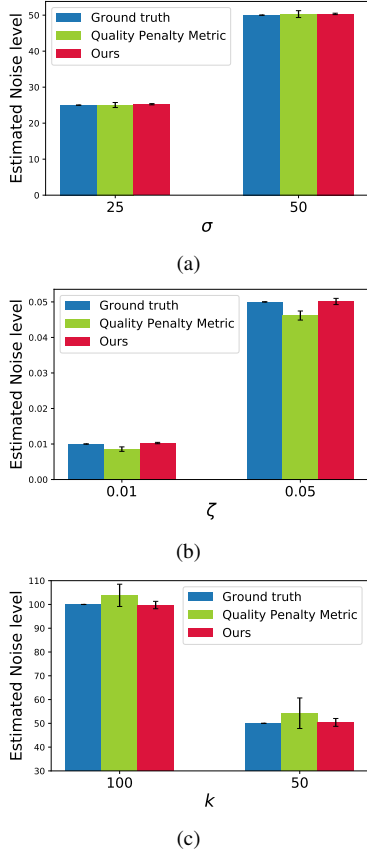


Figure 7. Estimated noise level parameters for each noise distribution in Kodak dataset. (a) Gaussian ($\sigma = 25$, and 50). (b) Poisson ($\zeta = 0.01$, and 0.05). (c) Gamma ($k = 100, 50$). The blue bars indicate the truth noise levels. The green bars and the red bars indicate that the average of estimated noise levels with the quality penalty metric in [10] and the proposed method, respectively.

Table 7. Ablation studies on score estimation using CBSD68 data (Poisson noise cases, $\zeta = 0.01$).

Component	Ours	Case1	Case2	Case3
EMA	✓	✓	✗	✗
GS	✓	✗	✓	✗
PSNR(dB)	32.53	32.41	32.23	32.03

J. Qualitative Results

We provide more examples of the denoising results by various methods on the AAPM CT dataset [17] as shown in Fig. 8. Similar to the results shown in the main paper, the improvements are consistent. In particular, other self-supervised approaches produce over-smooth denoised images, which produces the boundary structure of CT images in difference images. On the other hand, the proposed method provides similar results compared to target images and only generates noise components in the difference im-

ages.

K. Limitation and Negative Societal Impacts

While we provide a unified approach for noise distribution adaptive self-supervised image denoising, the method is not free of limitations. As the formulae for estimating of noise model and levels were derived from several approximations, it could fail in a real-world dataset. Furthermore, the noise model may not be described by Tweedie distribution in real environments.

As a negative societal impact, the failure of image denoising methods can lead to side effects. For example, removing both the noise and the texture of the medical images could lead to misdiagnosis.

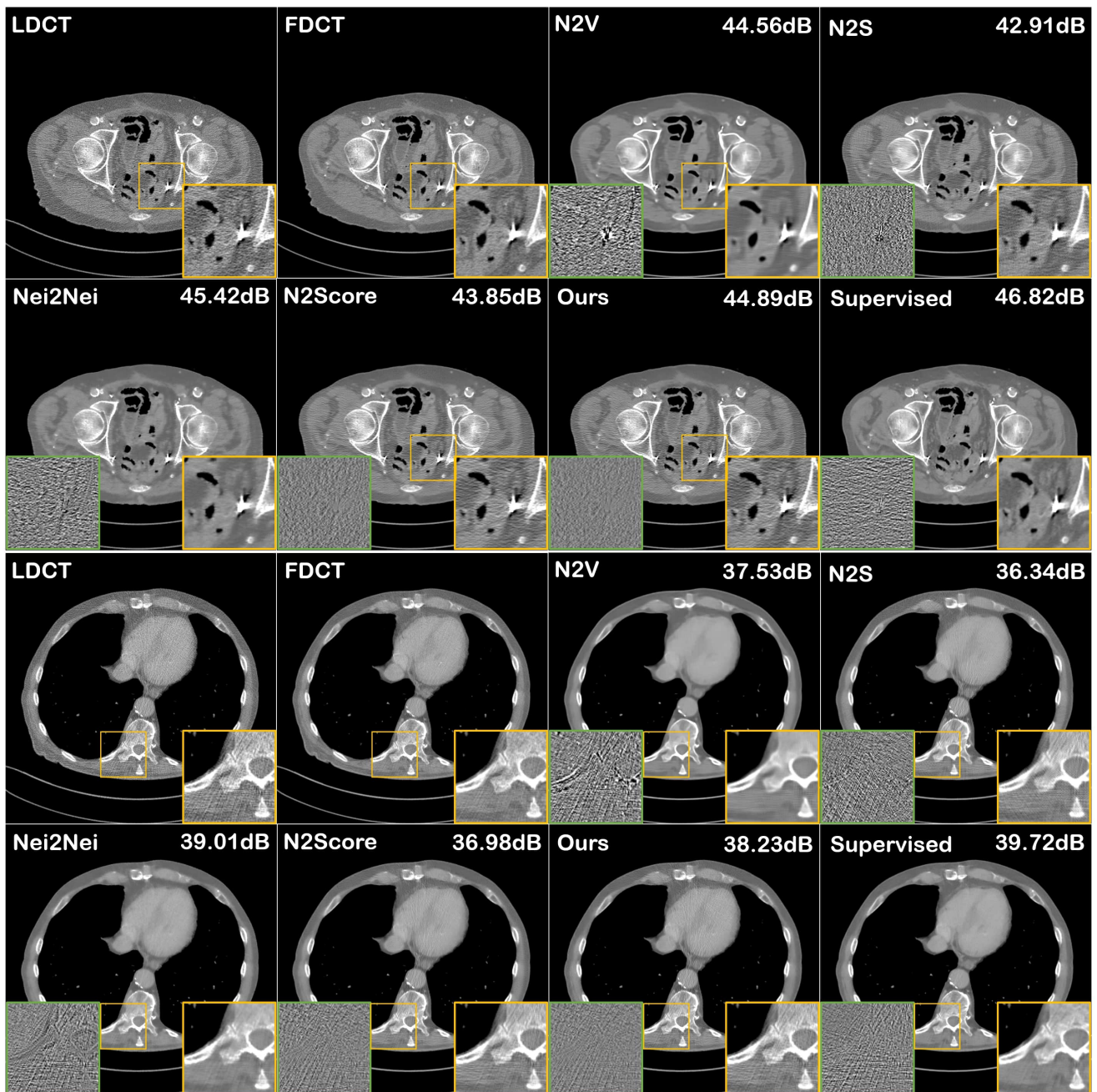


Figure 8. Denoising results of AAPM data using various methods. The yellow box and green box show the enlarged view of image and difference image between network input and output, respectively. The intensity window of CT image is $(-500,500)$ [HU] and the intensity window of difference is $(-200,200)$ [HU].